Evidence of cryptic methane cycling and non-methanogenic methylamine consumption in the sulfate-reducing zone of sediment in the Santa Barbara Basin, California

Sebastian J. E. Krause[1,a], Jiarui Liu[1], David J. Yousavich[1], DeMarcus Robinson[2], David W. Hoyt[3], Qianhui Qin[4], Frank Wenzhöfer[5,6,7], Felix Janssen[5,6], David L. Valentine[8], and Tina Treude[1,2]

[1]Department of Earth, Planetary and Space Sciences, University of California, Los Angeles, CA 90095, USA
[2]Department of Atmospheric and Ocean Sciences, University of California, Los Angeles, CA 90095, USA
[3]Pacific Northwest National Laboratory Environmental and Molecular Sciences Division, Richland, WA 99352, USA
[4]Interdepartmental Graduate Program in Marine Science, University of California, Santa Barbara, CA 93106, USA
[5]HGF-MPG Joint Research Group for Deep-Sea Ecology and Technology, Alfred Wegener Institute, Helmholtz Centre for Polar and Marine Research, Am Handelshafen 12, 27570 Bremerhaven, Germany
[6]HGF-MPG Joint Research Group for Deep-Sea Ecology and Technology, Max Planck Institute for Marine Microbiology, Celsiusstraße 1, 28359 Bremen, Germany
[7]Department of Biology, DIAS, Nordcee and HADAL Centres, University of Southern Denmark, 5230 Odense M, Denmark
[8]Department of Earth Science and Marine Science Institute, University of California Santa Barbara,
Santa Barbara, CA 93106, USA
[a]present address: Earth Research Institute, 6832 Ellison Hall, University of California Santa Barbara,
CA 93106-3060, USA

Correspondence: Sebastian J. E. Krause (sjkrause@ucsb.edu) and Tina Treude (ttreude@g.ucla.edu)

Abstract. The recently discovered cryptic methane cycle in the sulfate-reducing zone of marine and wetland sediment couples methylotrophic methanogenesis to anaerobic oxidation of methane (AOM). Here we present evidence of cryptic methane cycling activity within the upper regions of the sulfate-reducing zone, along a depth transect within the Santa Barbara Basin, off the coast of California, USA. The top 0–20 cm of sediment from each station was subjected to geochemical analyses and radiotracer incubations using ^{35}S–SO_4^{2-}, ^{14}C–mono-methylamine, and ^{14}C–CH_4 to find evidence of cryptic methane cycling. Methane concentrations were consistently low (3 to 16 µM) across the depth transect, despite AOM rates increasing with decreasing water depth (from max 0.05 nmol cm^{-3} d^{-1} at the deepest station to max 1.8 nmol cm^{-3} d^{-1} at the shallowest station). Porewater sulfate concentrations remained high (23 to 29 mM), despite the detection of sulfate reduction activity from ^{35}S–SO_4^{2-} incubations with rates up to 134 nmol cm^{-3} d^{-1}. Metabolomic analysis showed that substrates for methanogenesis (i.e., acetate, methanol and methylamines) were mostly below the detection limit in the porewater, but some samples from the 1–2 cm depth section showed non-quantifiable evidence of these substrates, indicating their rapid turnover. Estimated methanogenesis from mono-methylamine ranged from 0.2 to 0.5 nmol cm^{-3} d^{-1}. Discrepancies between the rate constants (K_1) of methanogenesis (from ^{14}C–mono-methylamine) and AOM (from either ^{14}C–mono-methylamine-derived ^{14}C–CH_4 or from directly injected ^{14}C–CH_4) suggest the activity of a separate, concurrent metabolic process directly metabolizing mono-methylamine to inorganic carbon. We conclude that the results presented in this work show strong evidence of cryptic methane cycling occurring within the top 20 cm of sediment in the Santa Barbara Basin. The rapid cycling of carbon between methanogenesis and methanotropy likely prevents major build-up of methane in the sulfate-reducing zone. Furthermore, our data suggest that methylamine is utilized by both methanogenic archaea capable of methylotrophic methanogenesis and non-methanogenic microbial

groups. We hypothesize that sulfate reduction is responsible for the additional methylamine turnover, but further investigation is needed to elucidate this metabolic activity.

1 Introduction

In anoxic marine sediment, methane is produced by microbial methanogenesis in the last step of organic carbon remineralization (Stephenson and Stickland, 1933; Thauer, 1998; Reeburgh, 2007). This methane is produced by groups of obligate anaerobic methanogenic archaea across the Euryarchaeota, Crenarchaeota, Halobacterota, and Thermoplasmatota phyla (Lyu et al., 2018). Methanogens can produce methane through three different metabolic pathways, using CO_2 (CO_2 reduction; e.g., hydrogenotrophic) (Reaction R1) and acetate (acetoclastic) (Reaction R2) and methylated substrates such as methyl sulfides, methanol, and methylamines (methylotrophic) (e.g., Reaction R3).

$$4H_2 + CO_2 \rightarrow CH_4 + 2H_2O \quad\quad\quad (R1)$$

$$CH_3COO^- + H^+ \rightarrow CO_2 + CH_4 \quad\quad\quad (R2)$$

$$4CH_3NH_2 + 2H_2O \rightarrow 3CH_4 + CO_2 + 4NH_4 \quad (R3)$$
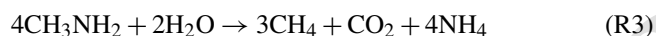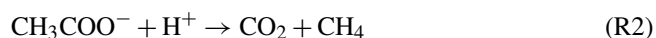
Classically, hydrogenotrophic and acetoclastic methanogenesis are dominant in deeper sulfate-free sediment (Jørgensen, 2000; Reeburgh, 2007). This distinct geochemical zonation is due to the higher free energy gained by sulfate-reducing bacteria within the sulfate reduction zone coupling sulfate reduction with hydrogen and/or acetate consumption in sulfate-rich sediment. Thus, sulfate-reducing bacteria tend to outcompete methanogenic archaea for hydrogen and acetate in shallower sediment layers in the presence of sulfate (Kristjansson et al., 1982; Winfrey and Ward, 1983; Lovley and Klug, 1986; Jørgensen, 2000). However, methylotrophic methanogenesis is known to occur within the sulfate-reducing zone. The activity of this process in the presence of sulfate reduction is possible because methylated substrates, such as methylamines, are non-competitive carbon sources for methanogens (Oremland and Taylor, 1978; Lovley and Klug, 1986; Maltby et al., 2016; Zhuang et al., 2016, 2018; Krause and Treude, 2021). Methylotrophic methanogenesis activity in the sulfate-reducing zone has been detected in a wide range of aquatic environments, such as coastal wetlands (Oremland et al., 1982; Oremland and Polcin, 1982; Krause and Treude, 2021), upwelling regions (Maltby et al., 2016), and eutrophic shelf sediment (Maltby et al., 2018; Xiao et al., 2018). Despite methylotrophic activity in the sulfate-reducing zone, methane concentrations are several orders of magnitude lower than methane concentrations found in deeper sediment zones where sulfate concentrations are depleted (Barnes and Goldberg, 1976; Dale et al., 2008b; Wehrmann et al., 2011; Beulig et al., 2018).

In anoxic marine sediment, anaerobic oxidation of methane (AOM) is an important methane sink that is typically coupled to sulfate reduction (Reaction R4) and mediated by a consortium of anaerobic methane-oxidizing archaea (ANME) and sulfate-reducing bacteria (Knittel and Boetius, 2009; Orphan et al., 2001; Michaelis et al., 2002; Boetius et al., 2000; Hinrichs and Boetius, 2002; Reeburgh, 2007).

$$CH_4 + SO_4^{2-} \rightarrow HCO_3^- + HS^- + H_2O \quad\quad (R4)$$

AOM occurring in the sulfate-reducing zone, fueled by concurrent methylotrophic methanogenesis activity, i.e., the cryptic methane cycle, could be the reason why methane concentrations are consistently low in sulfidic sediment (Krause and Treude, 2021; Xiao et al., 2017, 2018). These studies highlight the importance of the cryptic methane cycle on the global methane budget. However, the extent of our knowledge of cryptic methane cycle is restricted to a few aquatic environments. Thus, it is crucial to investigate the cryptic methane cycle in other aquatic environments to fully understand its impact on the global methane budget. In the present study we focus on organic-rich sediment below oxygen-deficient water in the Santa Barbara Basin (SBB), California.

Oxygen minimum zones (OMZs) are regions where high oxygen demand in the water column leads to a dramatic decline or even absence of dissolved oxygen (Wright et al., 2012; Paulmier and Ruiz-Pino, 2009; Wyrtki, 1962; Canfield and Kraft, 2022). In these environments, coastal upwelling of nutrients results in high phytoplankton growth, greatly enhancing organic matter loading and in turn creating a high metabolic oxygen demand during organic matter degradation in the water column. This enhanced respiration depletes oxygen faster than it is replenished (especially in poorly ventilated water bodies), which results in seasonal or continuous low oxygen conditions (Wyrtki, 1962; Helly and Levin, 2004; Wright et al., 2012; Levin et al., 2009). Sediment beneath OMZs is typically rich in organic matter supporting predominantly or exclusively anaerobic degradation processes, including methanogenesis (Levin, 2003; Rullkötter, 2006; Middelburg and Levin, 2009; Fernandes et al., 2022; Treude, 2011). Thus, sediment-underlying OMZs are a good candidate environments to investigate cryptic methane cycling.

Located within the Pacific Ocean, between the Channel Islands and the mainland of Santa Barbara, California, USA, the SBB is characterized as a thermally stratified, coastal marine basin with a maximum water column depth of approximately 590 m (Soutar and Crill, 1977; Arndt et al., 1990; Sholkovitz, 1973). Low oxygen concentrations ($< 10 \mu M$) are found in the bottom waters below the sill depth (~ 475 m) of the SBB (Sholkovitz, 1973; Reimers et al., 1996). The sediment in the SBB has an organic carbon content of 2%–6% (Schimmelmann and Kastner, 1993). These characteristics make the SBB a prime study site to find evidence of cryptic methane cycling.

Organic carbon sources for methylotrophic methanogenesis, such as methylamine, are ubiquitous in coastal marine

environments (Zhuang et al., 2018, 2016; Oren, 1990), including marine environments where OMZs exist (Ferdelman et al., 1997; Gibb et al., 1999). Methylamines are derived from osmolytes, such as glycine and betaine, and are synthesized by phytoplankton (Oren, 1990). However, the abundance of methylamines and how they may be driving cryptic methane cycling in anoxic sediment within OMZs is virtually unknown. Furthermore, the fate of methane from methylotrophic methanogenesis in the sulfate reduction zone is poorly constrained. Particularly, if cryptic methane cycling is active above the sulfate–methane transition zone, gross production and consumption of methane have likely been underestimated. Therefore, finding evidence for the cryptic methane cycle in the SBB is a necessary step towards understanding how carbon is cycled through the sediment of the SBB and other OMZs.

In the present study we report biogeochemical evidence of cryptic methane cycling in surface sediment (top ~ 15 cm) collected along a depth transect crossing the SBB. We applied the radiotracer method from Krause and Treude (2021) to trace the production of methane from mono-methylamine, followed by the anaerobic oxidation of methane to inorganic carbon. We combined this approach with standard radiotracer methods for the detection of AOM and sulfate reduction as well as with analyses of sediment porewater geochemistry.

2 Methods

2.1 Study site and sediment sampling

Sediment samples were collected during the R/V *Atlantis* expedition AT42-19 in fall 2019. Collection was achieved with polycarbonate push cores (30.5 cm long, 6.35 cm i.d.), which were deployed by the ROV *Jason* along a depth transect through the SBB. The depth transect selected for this particular study was the Northern Deposition Transect 3 (NDT3), with three stations (NDT3-A, NDT3-C, and NDT3-D), the Northern Depositional Radial Origin (NDRO), and the Southern Depositional Radial Origin (SDRO) station, located in the deepest part of the basin. Details on the stations' water column depths and near-seafloor oxygen concentrations are provided in Table 1.

Table 1. Water column depth, bottom water oxygen concentrations, and coordinates of each station sampled during this study.

Station	Depth (m)	Bottom water oxygen (μM)	Latitude	Longitude
SDRO	586	0	34.2011	−120.0446
NDRO	580	0	34.2618	−120.0309
NDT3-A	572	9.2	34.2921	−120.0258
NDT3-C	498	5	34.3526	−120.0160
NDT3-D	447	8	34.3625	−120.0150

After sediment collection, ROV push cores were returned to the surface by an elevator platform. Upon retrieval on board the R/V *Atlantis*, sediment samples were immediately transported to an onboard cold room (6 °C) for further processing of biogeochemical parameters (see details in Sect. 2.2).

2.2 Sediment porewater sampling and sulfate analysis

For porewater analyses, two ROV sediment push cores from each station were sliced in 1 cm increments in the top 10 cm of the sediment, followed by 2 cm increments below. During sediment sampling, ultra-pure argon was flushed over the sediment to minimize oxidation of oxygen sensitive species. The sliced sediment layers were quickly transferred to argon-flushed 50 mL plastic centrifuge vials and centrifuged at $2300 \times g$ for 20 min to extract the porewater. Subsequently, 2 mL of porewater was subsampled from the supernatant and frozen at -20 °C for shore-based sulfate analysis by ion chromatography (Metrohm 761) following Dale et al. (2015). Additional porewater (1 mL) was subsampled for the determination of the concentration of methylamine and other metabolic substrates (see Sect. 2.4).

2.3 Sediment methane and benthic methane flux analyses

Methane concentrations in the sediment were determined from a replicate ROV push core. Sediment was sliced at 1 cm increments in the top 10 cm, followed by 2 cm increments below. Two milliliters of sediment was sampled with a cut-off 3 mL plastic syringe and quickly transferred to 12 mL glass serum vials filled with 5 mL 5 % (w/w) NaOH solution. The vials were sealed immediately with a grey butyl rubber stopper and aluminum crimps, shaken thoroughly, and stored upside down at 4 °C. Methane concentrations in the headspace were determined shore-based using a gas chromatograph (Shimadzu GC-2015) equipped with a packed HayeSep-D column and flame ionization detector. The column was filled with helium as a carrier gas, flowing at 12 mL min^{-1} and heated to 80 °C. Methane concentrations in the environmental samples were calibrated against methane standards (Scott Specialty Gases) with a ± 5 % precision.

To determine methane flux out of the sediment and into the water column, 1–2 custom-built cylindrical benthic flux chambers (BFCs) (Treude et al., 2009) were deployed at each sampling station by the ROV *Jason*. The BFCs consist of a lightweight fiber-reinforced plastic frame, which holds a cylindrical polycarbonate chamber. Buoyant syntactic foam was attached to the feet of the frame to keep the BFCs from sinking too deep into the soft and poorly consolidated sediments, especially in the deeper stations. Water overlying the enclosed sediment was kept mixed with a stirrer bar rotating below the lid of the chamber. The BFCs were equipped with a syringe sampler holding seven 50 mL glass syringes (six

syringes for sample collection and one syringe for freshwater injection). Each sample syringe withdrew 50 mL of seawater from the chamber volume at pre-programmed time intervals. The seventh syringe was used to inject 50 mL of deionized water into the chamber shortly after deployment to calculate the volume from the change in salinity in the overlying seawater recorded by a conductivity sensor (type 5860, Aanderaa Data Instruments, Bergen, Norway), according to Kononets et al. (2021).

Seawater samples to determine the methane flux out of the sediments were collected in 26 mL serum glass bottles. The 26 mL serum bottles were acid cleaned and then combusted at 300 °C prior to BFC seawater sample collection. One to two pellets of solid NaOH were added into each empty 26 mL combusted serum bottle. All empty serum bottles were then flushed with ultra-pure nitrogen gas (Airgas Ultra High Purity Grade Nitrogen, Manufacturer Part no. UHP300) for 5 min and then sealed with autoclaved chlorobutyl stoppers and crimps. Lastly, a vacuum pump was used to evacuate the bottles to a pressure down to < 0.05 psi prior to sample collection.

Immediately after BFC recovery from the seafloor, approximately 20 mL of seawater sample was transferred into the pre-evacuated, acid cleaned, and combusted 26 mL glass serum bottles through the chlorobutyl stopper using a sterile 23G needle. Pressure within the serum bottle was equalized to atmospheric pressure with the introduction of UHP-grade nitrogen. Serum bottles were shaken to dilute the NaOH pellets, which terminated metabolic activity and forced the dissolved methane into the gas headspace. The serum bottles were reweighed after sample collection, to calculate the exact volume of the seawater sample. Methane concentrations in seawater collected from the BFCs were analyzed shipboard by gas chromatography according to Qin et al. (2022).

Total methane concentration in the headspace was calculated following the ideal gas law (Eq. 1):

$$n = \frac{PV}{RT} \cdot [\text{CH}_4] \cdot \frac{1}{V_{\text{SW}}}, \tag{1}$$

where n is the total molar concentration of methane, P is atmospheric pressure, V is the volume of the headspace of serum bottle (which is calculated by 26 mL subtracted by the volume of seawater sample), R is the ideal gas constant, T is temperature in kelvin (288.15 K), $[\text{CH}_4]$ is the methane measured by GC as percentage values in part per million, and V_{SW} is the volume of seawater in the serum vial. The volume of sampled seawater in each serum bottle was calculated by subtracting the mass of the empty serum bottle from the mass of the filled serum bottle, normalized by the density of seawater.

2.4 Determination of methanogenic substrates in porewater

To obtain sediment porewater concentrations of methanogenic substrates (methylamine, methanol, and acetate), 1 mL porewater was extracted from 1–2 and 9–10 cm depth sections at each station (see Sect. 2.2) and syringe-filtered (0.2 µm) into pre-combusted (350 °C for 3 h) amber glass vials (1.8 mL), which were then closed with a PTFE septa-equipped screw caps and frozen at −80 °C until analyses. Samples were analyzed at the Pacific Northwest National Laboratory, Environment and Molecular Sciences Division for metabolomic analysis using proton nuclear magnetic resonance (NMR). Prior to analysis, porewater samples were diluted by 10 % (v/v) with an internal standard (5 mM 2,2-dimethyl-2-silapentane-5-sulfonate-d6). All NMR spectra were collected using an 800 MHz Bruker Avance Neo (Tava), with a TCl 800/54 H&F/C/N-D-05 Z XT, and an QCl H-P/C/N-D-05 Z ET extended temperature range CryoProbe. The 1D 1H NMR spectra of all samples were processed, assigned, and analyzed by using the Chenomx NMR Suite 8.6 software with quantification based on spectral intensities relative to the internal standard. Candidate metabolites present in each of the complex mixture were determined by matching the chemical shift, J-coupling, and intensity information of experimental NMR signals against the NMR signals of standard metabolites in the Chenomx library. The 1D 1H spectra were collected following standard Chenomx data collection guidelines, employing a 1D NOESY presaturation experiment (noesypr1d) with 65536 complex points and at least 4096 scans at 298 K. Signal-to-noise ratios (S / N) were measured using MestReNova 14 with the limit of quantification equal to a S / N of 10 and the limit of detection equal to a S / N of 3. The 90° 1H pulse was calibrated prior to the measurement of each sample with a spectral width of 12 ppm and 1024 transients. The NOESY mixing time was 100 ms and the acquisition time was 4 s followed by a relaxation delay of 1.5 s, during which presaturation of the water signal was applied. Time domain free induction decays (72 114 total points) were zero-filled to 131 072 total points prior to Fourier transform.

2.5 Metabolic activity determinations

One replicate ROV sediment push core (hereafter "ROV rate push core") from each station was sub-sampled with three mini-cores (20 cm long, 2.6 cm i.d.) for radiotracer incubations according to the whole-core injection method (Jørgensen, 1978) to collect quantitative metabolic evidence (sulfate reduction, methanogenesis, methane oxidation) of cryptic methane cycling. The incubation methods are detailed below. Note that not enough sediment cores were collected at each station to perform replicate radiotracer experiments that

would have allowed addressing small-scale spatial variability in ex situ rates.

2.5.1 Sulfate reduction via ^{35}S–sulfate

Within the same day of collection, one mini-core from each ROV rate push core was used to determine sulfate-reduction rates. Radioactive carrier-free ^{35}S–sulfate (^{35}S–SO$_4^{2-}$; dissolved in Milli-Q water, injection volume 10 µL, activity 260 kBq, specific activity 1.59 TBq mg^{-1}) was injected into the mini-core at 1 cm increments and incubated at 6 °C in the dark following Jørgensen (1978). Injected sediment cores were stored vertically and incubated for ∼ 6 h at 6 °C in the dark. Incubations were stopped by slicing the sediment in 1 cm increments into 50 mL plastic centrifuge tubes containing 20 mL 20 % (w/w) zinc acetate solution. Each sediment sample was sealed and shaken thoroughly and stored at −20 °C to halt metabolic activity. For the control samples, sediments were added to zinc acetate solution prior to radiotracer injection. In the home laboratory, sulfate reduction rates were determined using the cold-chromium distillation method (Kallmeyer et al., 2004).

2.5.2 Methanogenesis and AOM via ^{14}C–mono-methylamine

This study aimed at determining the activity of methanogenesis from mono-methylamine (MG–MMA) and the subsequent anaerobic oxidation of the resulting methane to inorganic carbon by AOM (AOM–MMA). To accomplish this goal, a mini-core from each ROV rate push core was injected with radiolabeled ^{14}C–mono-methylamine (^{14}C–MMA; dissolved in 1 mL water, injection volume 10 µL, activity 220 kBq, specific activity 1.85–2.22 GBq mmol^{-1}) similar to Sect. 2.5.1. After 24 h, the incubation was terminated by slicing the sediment at 1 cm increments into 50 mL wide mouth glass vials filled with 20 mL of 5 % NaOH. Five killed control samples were prepared by transferring approximately 5 mL of extra sediment from each station into 50 mL wide mouth vials filled with 20 mL of 5 % NaOH prior to radiotracer addition. Sample vials and vials with killed controls were immediately sealed with butyl rubber stoppers and aluminum crimps and shaken thoroughly for 1 min to ensure complete biological inactivity. Vials were stored upside down at room temperature until further processing. In the home laboratory, methane production from ^{14}C–MMA by MG–MMA and subsequent oxidation of the produced ^{14}C–methane (^{14}C–CH$_4$) by AOM–MMA were determined according to the adapted radiotracer method outlined in Krause and Treude (2021).

To account for ^{14}C–MMA potentially bound to mineral surfaces (Wang and Lee, 1993, 1994; Xiao et al., 2022), we determined the ^{14}C–MMA recovery factor (RF) for the sediment from the stations NDT3-C, NDT3-D, and NDRO according to Krause and Treude (2021).

Metabolic rates of MG–MMA were calculated according to Eq. (2). Note that natural concentrations of MMA in the SBB sediment porewater were either below detection or detectable but below the quantification limit (< 10 µM) (Supplement Table S1). Therefore, MMA concentrations were assumed to be 3 µM to calculate the ex situ rate of MG–MMA (Eq. 2).

$$\text{MG–MMA} = \frac{a_{\text{CH}_4} + a_{\text{TIC}}}{a_{\text{CH}_4} + a_{\text{TIC}} + \left[\frac{a_{\text{MMA}}}{\text{RF}}\right]} \cdot [\text{MMA}] \cdot \frac{1}{t}, \qquad (2)$$

where MG–MMA is the rate of methanogenesis from mono-methylamine (nmol cm^{-3} d^{-1}); a_{CH_4} is the radioactive methane produced from methanogenesis (CPM); a_{TIC} is the radioactive total inorganic carbon produced from the oxidation of methane (CPM); a_{MMA} the residual radioactive mono-methylamine (CPM); RF is the recovery factor (Krause and Treude, 2021); [MMA] is the assumed mono-methylamine concentrations in the sediment (nmol cm^{-3}); t is the incubation time (d). ^{14}C–CH$_4$ and ^{14}C–TIC sample activity was corrected by respective abiotic activity determined in killed controls.

Results from the ^{14}C–MMA incubations were also used to estimate the AOM–MMA rates according to Eq. (3):

$$\text{AOM–MMA} = \frac{a_{\text{TIC}}}{a_{\text{CH}_4} + a_{\text{TIC}}} \cdot [\text{CH}_4] \cdot \frac{1}{t}, \qquad (3)$$

where AOM–MMA is the rate of anaerobic oxidation of methane based on methane produced from MMA (nmol cm^{-3} d^{-1}); a_{TIC} is the produced radioactive total inorganic carbon (CPM); a_{CH_4} is the residual radioactive methane (CPM); [CH$_4$] is the sediment methane concentration (nmol cm^{-3}); t is the incubation time (d). ^{14}C–TIC activity was corrected by abiotic activity determined by replicate dead controls.

2.5.3 Anaerobic oxidation of methane via ^{14}C–methane

AOM rates from ^{14}C–CH$_4$ (AOM–CH$_4$) were determined by injecting radiolabeled ^{14}C–CH$_4$ (dissolved in anoxic Milli-Q, injection volume 10 µL, activity 5 kBq, specific activity 1.85–2.22 GBq mmol^{-1}) into one mini-core from each ROV rate core at 1 cm increments similar to Sect. 2.5.1. Incubations of the mini-cores were stopped after ∼ 24 h similar to Sect. 2.5.2. In the laboratory, AOM–CH$_4$ was analyzed using oven combustion (Treude et al., 2005) and acidification/shaking (Joye et al., 2004). The radioactivity was determined by liquid scintillation counting. AOM–CH$_4$ rates were calculated according to Eq. (3).

2.5.4 Rate constants for AOM–CH$_4$, MG–MMA, and AOM–MMA

Metabolic rate constants (k) for AOM–CH$_4$, MG–MMA, and AOM–MMA were calculated for relative turnover comparisons using the experimental data determined by Sect. 2.5.2

and 2.5.3. The rate constants consider the metabolic reaction products divided by the sum of the reaction reactants and products and divided by the incubation time. The metabolic rate constants for AOM–CH_4, MG–MMA, and AOM–MMA were calculated according to Eq. (4):

$$k = \frac{a_{products}}{a_{products} + a_{reactants}} \cdot \frac{1}{t}, \tag{4}$$

where k is the metabolic rate constant (d^{-1}); $a_{products}$ is the radioactivity (CPM) of the metabolic reaction products; $a_{reactants}$ is the radioactivity (CPM) of the metabolic reaction reactants; t is time in days.

3 Results

3.1 Sediment biogeochemistry

At most stations, porewater methane concentrations in the top 10–20 cm of sediment fluctuated between 3 and 13 μM with no clear trend (Fig. 1a, e, i, m, and q). At NDRO, methane steadily increased below 12 cm, reaching 16 μM at 14–15 cm (Fig. 1e). Methane concentrations determined in water samples from the BFC incubations revealed only minor fluctuations over time with no clear trends, suggesting no net fluxes of methane into or out of the sediment at all stations (Fig. S1 in the Supplement). It is notable, however, that the BFCs captured higher methane concentrations (350–800 nM) in the supernatant of station SDRO, NDRO, and NDT3-A compared to NDT3-C and NDT3-D (< 130 nM). Sulfate concentrations showed no strong decline with depth at any station (except maybe a weak tendency at SDRO and NDT3-A) and fluctuated between 23 and 30 mM in the sampled top 10–20 cm (Fig. 1a, e, i, m, and q).

Table S1 provides porewater concentrations of organic carbon sources from the metabolomic analysis, as measured by NMR, that are known to support methanogenesis. Methylamine was detected at SDRO and NDT3-A (1–2 cm), but those concentrations were below the quantification limit (10 μM). Otherwise, methylamine was below detection (< 3 μM) for all other samples. Similarly, methanol was detected but below quantification at NDT3-A (1–2 cm) but otherwise below detection. Acetate was at a quantifiable level (21 μM) at NDT3-A (1–2 cm) but was otherwise either below quantification (SDRO, 1–2 cm; NDRO, 1–2 cm) or below detection.

3.2 AOM from ^{14}C–methane and sulfate reduction from ^{35}S–sulfate

Figure 1b, f, j, n, and r depict ex situ rates of AOM–CH_4 and sulfate reduction from the radiotracer incubations with ^{14}C–methane and ^{35}S–sulfate in sediment mini-cores, respectively. AOM–CH_4 activity tended to increase with decreasing water depth in the top 5 cm of the sediment (from max

0.05 nmol cm^{-3} d^{-1} at NDRO to max 4.5 nmol cm^{-3} d^{-1} at NDT3-D), while rates were either negligible (SDRO, NDRO, NDT3-A) or < 1 nmol cm^{-3} d^{-1} (NDT3-C, NDT3-D) for depths > 5 cm. Where peaks in AOM were present (SDRO, NDT3-C, NDT3-D) they were always located in the top 0–1 cm sediment layer.

Sulfate reduction activity was detected throughout all sediment cores with the highest rates mostly at 0–1 cm, followed by a decrease with increasing sediment depth. The highest individual sulfate reduction peaks were found at NDRO, NDT3-A, and NDT3-C (120, 85, and 133 nmol cm^{-3} d^{-1}). At NDT3-D sulfate reduction rates varied between 14 and 45 nmol cm^{-3} d^{-1} throughout the core with no clear trend. Note that sulfate reduction data are missing for 0–5 cm at SDRO, due to post-cruise analytical issues. Here, rates gradually decreased from 52 to 10 nmol cm^{-3} d^{-1} below 5 cm.

3.3 Methanogenesis and AOM from ^{14}C–mono-methylamine

3.3.1 ^{14}C–MMA recovery from sediment

RF values determined in sediments from NDRO, NDT3-C, and NDT3-D stations (see Sect. 2.5.2) were 0.93, 0.84, and 0.75, respectively. They were used to correct MG–MMA rates at each station of the study. Note that no RF values were determined for SDRO or the NDT3-A. We applied RF values from NDRO and NDT3-C, respectively, instead.

3.3.2 MG–MMA and AOM–MMA

Figure 1c, g, k, o, and s show ex situ rates of MG–MMA and AOM–MMA, assuming a natural MMA concentration of 3 μM (see Sect. 2.5.2). At SDRO, NDRO, and NDT3-A, MG–MMA ranged between 0.27 and 0.45 nmol cm^{-3} d^{-1} throughout the sediment core without trend (Fig. 1c, g, and k). At NDT3-C MG–MMA ex situ rates were lower ranging between 0.007 and 0.3 nmol cm^{-3} d^{-1} without any pattern (Fig. 1o). At NDT3-D, MG–MMA sharply increased from 0.05 nmol cm^{-3} d^{-1} at 0–1 cm to 0.34 nmol cm^{-3} d^{-1} at 1–2 cm. MG–MMA then decreased slightly to 0.2 nmol cm^{-3} d^{-1} between 2 and 9 cm, before increasing to 0.5 nmol cm^{-3} d^{-1} at the bottom of the core (Fig. 1s).

AOM–MMA rates were 1 to 2 orders of magnitude higher than MG–MMA rates and 1 to 4 orders of magnitude higher than AOM–CH_4 rates (Fig. 1c, g, k, o, s). At SDRO, NDRO, NDT3-A, and NDT3-C, AOM–MMA ex situ rates ranged between 5.3 and 10 nmol cm^{-3} d^{-1} (unless zero) with no trend (Fig. 1c, g, k, and o). At NDT3-D, AOM–MMA rates decreased from 15.9 nmol cm^{-3} d^{-1} at 1–2 cm to 9 nmol cm^{-3} d^{-1} at 11–12 cm (Fig. S1). At all stations, some sediment intervals showed no biological net AOM–MMA activity (Fig. 1c, g, k, o, s). In these sediment intervals, the ^{14}C–
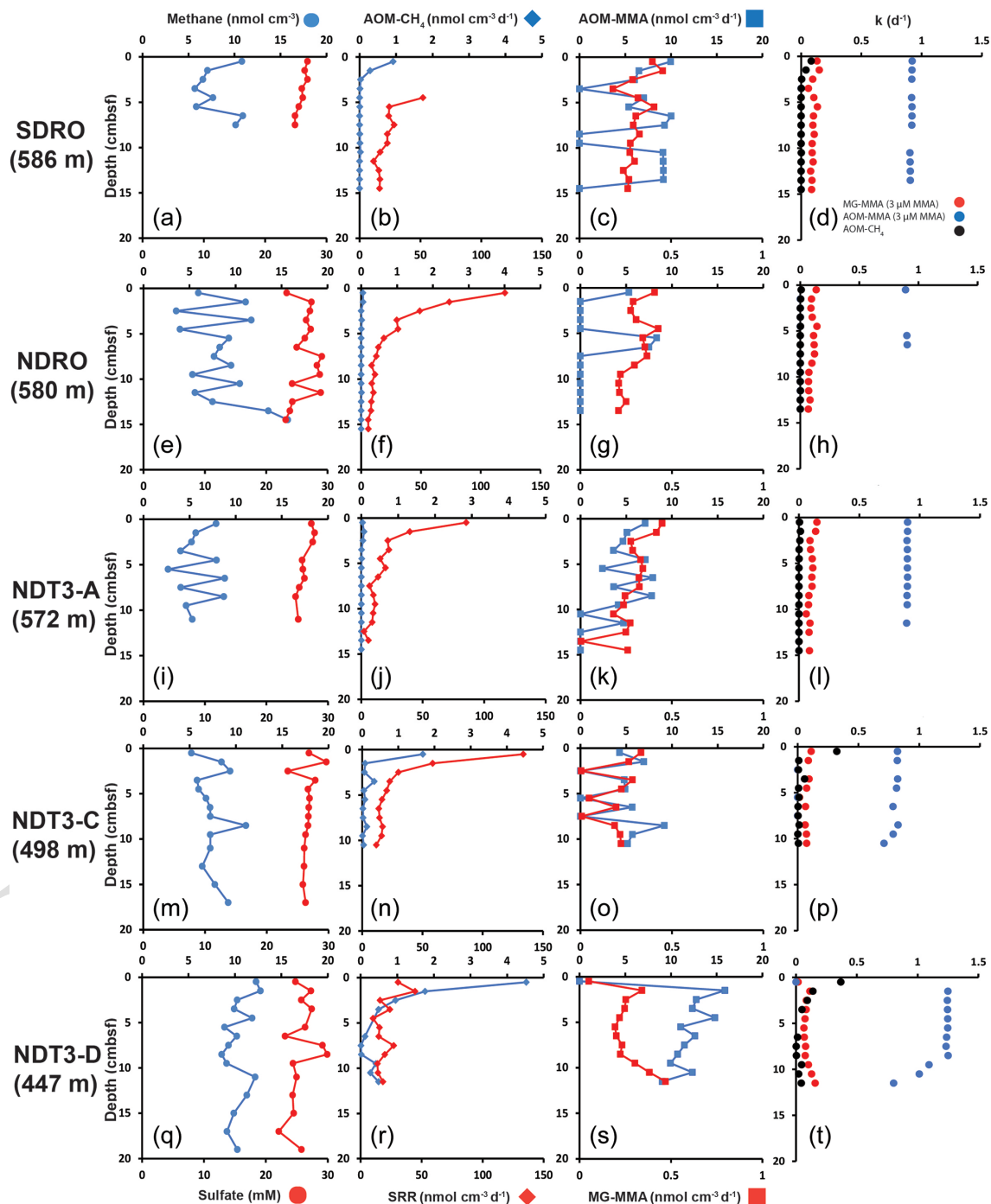
Figure 1. Depth profiles of biogeochemical parameters in sediment across the depth transect of the Santa Barbara Basin. **(a)**, **(e)**, **(i)**, **(m)**, and **(q)**: sediment methane and porewater sulfate; **(b)**, **(f)**, **(j)**, **(n)**, and **(r)**: AOM–CH_4 and sulfate reduction (determined from direct injection of ^{14}C–CH_4 and ^{35}S–sulfate, respectively); **(c)**, **(g)**, **(k)**, **(o)**, and **(s)**: AOM–MMA and MG–MMA (determined from direct injection of ^{14}C–MMA); **(d)**, **(h)**, **(l)**, **(p)**, and **(t)**: rate constants for AOM–CH_4, MG–MMA, and AOM–MMA.

TIC activity was statistically not different from the average plus the standard deviation of the killed control samples.

3.4 Rate constants for MG–MMA, AOM–MMA, and AOM–CH$_4$

Figure 1d, h, l, p, and t show the rate constants (k) for MG–MMA, AOM–MMA, and AOM–CH$_4$ for the comparison of relative radiotracer turnover. At all stations, MG–MMA rate constants were between 0.01 and 0.15 d^{-1}. AOM–CH$_4$ rate constants ranged between 0.0009 and 0.3 d^{-1}. Rate constants for AOM–MMA, however, were considerably higher than MG–MMA and AOM–CH$_4$ with values ranging between 0.7 and 1.2 d^{-1}. Most rate constants remained constant over depth, with the exemption of AOM–MMA at station NDT3-C and NDT3-D (Fig. 1p and t), which showed a steady decrease below 9 cm.

4 Discussion

4.1 Evidence of cryptic methane cycling

The aim of the present study was to check for the existence of cryptic methane cycling in SBB surface sediments by presenting evidence for the concurrent activity of sulfate reduction, AOM, and methanogenesis through radiotracer incubations (^{35}S–SO$_4^{-2}$, ^{14}C–CH$_4$, and ^{14}C–MMA, respectively). Our study confirmed indeed that the three processes co-exist at all investigated stations (Fig. 1). The most prominent concurrent metabolic activity was evident from activity peaks near the sediment–water interface at station NDT3-C (Fig. 1n and o). We suggest the concurrent peaking was stimulated by the availability of fresh, i.e., recently deposited, organic matter coinciding with low oxygen concentrations in the bottom water (Table 1). Fresh organic material likely provided a source for both organoclastic sulfate reduction and methylotrophic methanogenesis and indirectly (i.e., linked to the methane produced) for AOM coupled to either nitrate, iron, or sulfate reduction. Low oxygen concentrations offered favorable conditions for anaerobic processes in the surface sediment. At the remaining stations (SDRO, NDRO, SDT3-A, SDT3-D; Fig. 1), metabolic activity of all three processes was also confirmed near the sediment surface (with the exemption of the missing data for sulfate reduction at SDRO), but they not always depicted rate peaks (particularly not for AOM–CH$_4$).

Methane detected in the sulfate-rich sediment (Fig. 1a, e, i, m, q) was likely produced by methylotrophic methanogenesis utilizing non-competitive substrates within the sulfate-reducing zone (Oremland and Taylor, 1978; King et al., 1983; Maltby et al., 2016, 2018; Reeburgh, 2007), which is also indicated by the production of methane from our ^{14}C–MMA incubations. It is interesting to note that methane concentrations remained relatively constant around 5 to 12 µM, while AOM–CH$_4$ tended to increase with decreasing water depth.

This pattern suggests that the partial pressure of methane was likely determined by thermodynamic equilibrium between methanogenesis and AOM (compare, e.g., with Conrad, 1999).

The finding of non-linear methane concentrations in surface sediments is against the general view that methane concentrations above the sulfate–methane transition zone show a linear, diffusion-controlled decline towards the sediment–water interface, where methane escapes into the water column (Reeburgh, 2007). We argue that the non-linear methane trends we observe in the present study is an indication for simultaneous methane production and consumption, i.e., cryptic methane cycling, as evident from our radiotracer experiments.

As there is considerable methanogenic activity even at the sediment–water interface (0–1 cm) at all stations, aside from station NDT3-D (Fig. 1c, g, k, o, s), it is conceivable that some methane could diffuse into the water column where it may be oxidized by either aerobic or anaerobic oxidation processes (depending on the presence or absence of oxygen, respectively) before emission into the atmosphere (Reeburgh, 2007). However, benthic chamber incubations at the SBB stations did not indicate a release of methane into the water column (Fig. S1), emphasizing the importance of cryptic methane cycling for preventing the build-up of methane in the surface sediment and its emission into the water column.

4.2 Rapid turnover of metabolic substrates

Natural porewater MMA concentrations were mostly below detection (< 3 µM); however, in porewater close to the sediment–water interface of SDRO and NDT3-A, MMA was detected but below the quantification limit (< 10 µM) (Table S1). Although we are unable to report definitive MMA concentrations, we can bracket the MMA concentrations in a range between 3 and 10 µM. The bracketed MMA concentrations are about 1 to 2 orders of magnitude higher than what has been reported from porewater at other locations. For example, studies of sediment porewater off the coast of Peru found MMA concentrations to be ~ 0.15 µM (Wang and Lee, 1990). Similarly, in sediment porewater collected from Buzzards Bay, Massachusetts, and in the eastern tropical North Pacific Ocean, MMA concentrations were either present at trace amounts or below detection limit (< 0.05 µM) (Lee and Olson, 1984). Detectable but low methylamine concentrations in the porewater found in our study could imply that methylamines are rapidly consumed by microbiological processes and/or removed from the porewater through binding to minerals (Wang and Lee, 1990, 1993; Xiao et al., 2022). Our study provided support for both hypotheses as we detected the biological potential for MMA consumption via radiotracer (^{14}C–MMA) experiments (Fig. 1) and detected the binding of 7 %–25 % the injected ^{14}C–MMA to sediment (see Sect. 3.3.1).

Porewater methanol concentrations in the present study were also mainly below detection, except for one sample, where it was not quantifiable (NDT3-A, 1–2 cm; Table S1). In the marine environment, methanol is known to be a non-competitive substrate for methanogenesis (King et al., 1983; Oremland and Taylor, 1978). However, a recent study demonstrated that methanol is a carbon source for a wide variety of metabolisms, including sulfate-reducing and denitrifying bacteria, as well as aerobic and anaerobic methylotrophs (Fischer et al., 2021), which could all be present in the SBB sediments keeping methanol concentrations low. Acetate was also detected in the metabolomic analysis but mostly below quantification (except NDT3-A, 1–2 cm; Table S1). Acetate is formed through fermentation reactions or through homoacetogenesis (Jørgensen, 2000; Ragsdale and Pierce, 2008). It is a favorable food source for many bacteria and archaea such as sulfate reducers and methanogens (Jørgensen, 2000; Conrad, 2020), which would explain its low concentration in the SBB sediments. Low concentrations of the abovementioned metabolites are likely signatures of rapid metabolic turnover, similar to what has been described for microbial utilization of hydrogen in sediment (Conrad, 1999; Hoehler et al., 2001). In this situation, metabolites would be kept at a steady-state concentration close to the thermodynamic equilibrium of the respective consumers.

4.3 Competitive methylamine turnover by non-methanogenic pathways

Large disparities were found between AOM rates determined from the direct injection of ^{14}C–CH_4 (i.e., AOM–CH_4) and AOM determined from the production of ^{14}C–TIC in the ^{14}C–MMA incubations (i.e., AOM–MMA). AOM–CH_4 was roughly 1–2 orders of magnitude lower compared to AOM–MMA (compare Fig. 1b/c, f/g, j/k, n/o, r/s), indicating that AOM rates determined via ^{14}C–MMA incubations were overestimated. We hypothesize that this disparity is the result of the direct conversion of ^{14}C–MMA to ^{14}C–TIC by processes other than AOM coupled to MG–MMA. Any process converting ^{14}C–MMA directly to ^{14}C–TIC would inflate the rate constant only slightly for MG–MMA but dramatically for AOM–MMA (see Eqs. 6, 7, and 8). Figure 1d, h, l, p, and t confirm that the rate constants for AOM–MMA are 1 to 2 orders of magnitude higher compared to AOM–CH_4 and MG–MMA. We interpret the difference in these rate constants to strongly suggests that the ^{14}C–TIC detected in the analysis of samples incubated with ^{14}C–MMA must result not only from AOM involved in the cryptic methane cycle but also from direct methylamine oxidation by a different anaerobic methylotrophic metabolism that could not be disambiguated using the adapted radiotracer method.

Methylamines are the simplest alkylated amine. They are derived from the degradation of choline and betaine found in plant and phytoplankton biomass (Oren, 1990; Taubert et al., 2017). The molecules are ubiquitously found in saline and hypersaline conditions in the marine environment (Zhuang et al., 2016; Zhuang et al., 2017; Mausz and Chen, 2019). The importance of methylamine as a nitrogen and carbon source for microbes to build biomass has been well documented (Taubert et al., 2017; Capone et al., 2008; Anthony, 1975; Mausz and Chen, 2019). Methylamines can be metabolized by aerobic methylotrophic bacteria (Taubert et al., 2017; Chistoserdova, 2015; Hanson and Hanson, 1996) and by methylotrophic methanogens anaerobically (Chistoserdova, 2015; Thauer, 1998). Based on the data reported in the present study, we suggest that, in addition to methylotrophic methanogenesis, sulfate reduction was involved in MMA consumption in surface sediment of the SBB.

Recent literature does implicate anaerobic methylamine oxidation by sulfate reduction. For example, Cadena et al. (2018) performed in vitro incubations with microbial mats collected from a hypersaline environment with various competitive and non-competitive substrates including trimethylamine. Microbial mats incubated with trimethylamine stimulated considerable methane production, but after 20 d, H_2S began to accumulate and plateaued after 40 d, suggesting that trimethylamine is not exclusively shuttled to methylotrophic methanogenesis. The molecular data reported in Cadena et al. (2018), however, could not identify a particular group of sulfate-reducing bacteria that proliferated by the addition of trimethylamine. Instead, their molecular data suggested potentially other, non-sulfate-reducing bacteria, such as those in the family Flavobacteriaceae, to be responsible for trimethylamine turnover.

Zhuang et al. (2019) investigated heterotrophic metabolisms of C1 and C2 low molecular weight compounds in anoxic sediment collected in the Gulf of Mexico. Sediment was incubated with a variety of ^{14}C radiotracers alone and in combination with molybdate, a known sulfate reducer inhibitor, to elucidate the metabolic turnover of low molecular weight compounds, including ^{14}C-labeled trimethylamine. Their results showed that although methylamines did stimulate methane production, radiotracer incubations with molybdate and methylamine demonstrated the inhibition of direct oxidation of ^{14}C–methylamine to ^{14}C–CO_2, suggesting that methylamines were simultaneously oxidized to inorganic carbon by non-methanogenic microorganisms. This finding further suggests a competition between methanogens and sulfate-reducing bacteria for methylamine; however, the authors could not rule out AOM as a potential contributor to the inorganic carbon pool.

Kivenson et al. (2021) discovered dual genetic code expansion in sulfate-reducing bacteria from sediment within a deep-sea industrial waste dumpsite in the San Pedro Basin, California, which potentially allows the metabolization of trimethylamine. The authors expanded their study to revisit metagenomic and metatranscriptomic data collected from the Baltic Sea and in the Columbia River estuary and found expression of trimethylamine methyltransferase in Deltaproteobacteria. This result suggested that a trimethy-

lamine metabolism does exist in sulfate-reducing bacteria, which was enabled by the utilization of genetic code expansion. Furthermore, their results also suggest that trimethylamine could be the subject of competition between sulfate-reducing bacteria and methylotrophic methanogens.

Although the evidence of sulfate-reducing bacteria playing a larger role in methylamine utilization is growing, there are other methylotrophic microorganisms in anaerobic settings that could also be responsible for degrading methylamines. De Anda et al. (2021) discovered and classified a new phylum called Brockarchaeota. The study reconstructed archaeal metagenome-assembled genomes from sediment near hydrothermal vent systems in the Guaymas Basin, Gulf of California, Mexico. Their findings showed that some Brockarchaeota are capable of assimilating trimethylamines, by way of the tetrahydrofolate methyl branch of the Wood–Ljungdahl pathway and the reductive glycine pathway, bypassing methane production in anoxic sediment.

Farag et al. (2021) found genomic evidence of a novel Asgard phylum called Sifarchaeota in deep marine sediment off the coast of Costa Rica. The study used comparative genomics to show a cluster, *Candidatus* Odinarchaeota within the Sifarchaeota phylum, which contains genes encoding for an incomplete methanogenesis pathway that is coupled to the carbonyl branch of the Wood–Ljungdahl pathway. The results suggest that this cluster could be involved with utilizing methylamines. The Sifarchaeota metagenome-assembled genomes results found genes for nitrite reductase and sulfate adenylyltransferase and phosphoadenosine phosphosulfate reductase, indicating Sifarchaeota could perform nitrite and sulfate reduction. However, their study did not directly link nitrite and sulfate reduction to the utilization of methylamines by Sifarchaeota.

Molecular analysis was not performed in the present study; therefore, we are unable to directly link sulfate-reducing or any other heterotrophic bacteria to the direct anaerobic oxidation of methylamine in the SBB. Future work should combine available geochemical and molecular tools to piece together the complexity of metabolisms involved with methylamine turnover and how it may affect the cryptic methane cycle. We note that there appears to be a growing paradigm shift in the understanding of the utilization of non-competitive substrates in anoxic sediment by sulfate-reducing bacteria and methylotrophic methanogens (including other supposedly non-competitive methanogenic substrates like methanol; Sousa et al., 2018; Fischer et al., 2021). Apparently, methanogens are in fact able to convert these substrates into methane in the presence of their competitors. Which factors provide them this capability should be the subject of future research.

4.4 Implications for cryptic methane cycling in SBB

The SBB is known to have a network of hydrocarbon cold seeps, where methane and other hydrocarbons are released from the lithosphere into the hydro- and atmosphere either perennially or continuously (Hornafius et al., 1999; Leifer et al., 2010; Boles et al., 2004). The migration of methane and other hydrocarbons vertically into the hydrosphere occur along channels that are focused and permeable, such as fault lines and fractures (Moretti, 1998; Smeraglia et al., 2022). Local tectonics and earthquakes could create new fault lines or fractures that reshape or redisperse less permeable sediments, which may open or close migration pathways for hydrocarbons, including methane (Smeraglia et al., 2022). In fact it has been shown that hydrocarbons move much more efficiently through faults when the region in question is seismically active on timescales < 100 000 years (Moretti, 1998). Given the current and historical seismic activity (Working Group on California Earthquake Probabilities, 1995) and faulting (Boles et al., 2004) within and surrounding the SBB, it is conceivable that hydrocarbon seep patterns and seepage pathways could also shift over time. A potential consequence of this shifting in the SBB is that methane seepage could spontaneously flow through prior non-seep surface sediment. The fate of this methane would then fall on the methanotrophic communities that are part of the cryptic methane cycle. However, it is not well understood how quickly anaerobic methanotrophs could handle this shift due to their extremely slow growth rates (Knittel and Boetius, 2009; Wilfert et al., 2015; Nauhaus et al., 2007; Dale et al., 2008a). After gaining a better understanding of cryptic methane cycling in the SBB presented in this study, a hypothesis worth testing in future studies is whether cryptic methane cycling based on methylotrophic methanogenesis primes surface sediments to respond faster to increases in methane transport through the sediment.

5 Conclusions

In the present study, we set about to find evidence of cryptic methane cycling in the sulfate-reduction zone of sediment along a depth transect in the oxygen-deficient SBB using a variety of biogeochemical analytics. We found that, within the top 10–20 cm, low methane concentrations were present within sulfate-rich sediment and in the presence of active sulfate reduction. The low methane concentrations were attributed to the balance between methylotrophic methanogenesis and subsequent consumption of the produced methane by AOM. Our results therefore provide strong evidence of cryptic methane cycling in the SBB. We conclude that this important, yet overlooked, process maintains low methane concentrations in surface sediments of this OMZ, and future work should consider cryptic methane cycling in other OMZs to better constrain carbon cycling in these expanding marine environments.

Our radiotracer analyses further indicated microbial activity that oxidizes monomethylamine directly to CO_2, thereby bypassing methane production. Based off the sulfate reduc-

tion activity and methylamine consumption to CO_2 detected in this study and the metagenomic clues presented in the literature, we hypothesize that sulfate reduction may also be supported by methylamines. Our study highlights the metabolic complexity and versatility of anoxic marine sediment near the sediment–water interface within the SBB. Future work should consider how methylamines are consumed by different groups of bacteria and archaea, how methylamine utility by other anaerobic methylotrophs affects the cryptic methane cycle, and evaluate whether potential environmental changes affect the cryptic methane cycle activity.

Data availability. Porewater sulfate concentrations and sulfate reduction rates are accessible through the Biological & Chemical Oceanography Data Management Office (BCO-DMO) under the following DOIs: https://doi.org/10.26008/1912/bco-dmo.867007.1 (Treude and Valentine, 2022a), https://doi.org/10.26008/1912/bco-dmo.867113.1 (Treude and Valentine, 2022b) and https://doi.org/10.26008/1912/bco-dmo.867221.1 (Treude and Valentine, 2022c).
Sediment methane concentrations and rates and rate constant data of AOM and methanogenesis can be found in Table S2.

Supplement. The supplement related to this article is available online at: https://doi.org/10.5194/bg-20-1-2023-supplement.

Author contributions. SJEK and TT designed the study; SJEK, JL, DJY, DR, DWH, QQ, FW, and FJ performed experiments and made measurements; SJEK, JL, DJY, DR, DWH, QQ, FW, FJ, DLV, and TT analyzed the data; SJEK and TT wrote the manuscript draft with input from all co-authors.

Competing interests. At least one of the (co-)authors is a member of the editorial board of *Biogeosciences*. The peer-review process was guided by an independent editor, and the authors also have no other competing interests to declare.

Acknowledgements. We thank the captain and crew of R/V *Atlantis*, the crew of ROV Jason, the crew of AUV *Sentry*, and the science party of the research cruise AT42-19 for their technical and logistical support. This work was supported by the National Science Foundation NSF award no. EAR-1852912, OCE-1829981 (to Tina Treude), and OCE-1830033 (to David L. Valentine). The NMR experiments in this study were performed under a limited-scope project awarded to Tina Treude (proposal no. 51757; https://doi.org/10.46936/ltds.proj.2020.51757/60006896) using the Environmental Molecular Sciences Laboratory (https://ror.org/04rc0xn13, last access: 20 February 2021), a Department of Energy (DOE) Office of Science User Facility sponsored by the Biological and Environmental Research program under contract no. DE-AC05-76RL01830.

Financial support. This research has been supported by the National Science Foundation (grant nos. 1852912 and 1829981).

Review statement. This paper was edited by Jack Middelburg and reviewed by two anonymous referees.

References

Anthony, C.: The biochemistry of methylotrophic micro-organisms, Sci. Prog., 62, 167–206, 1975.

Arndt, S., Lange, C. B., and Berger, W. H.: Climatically controlled marker layers in Santa Barbara Basin sediments and fine-scale core-to-core correlation, Limnol. Oceanogr., 35, 165–173, 1990.

Barnes, R. and Goldberg, E.: Methane production and consumption in anoxic marine sediments, Geology, 4, 297–300, 1976.

Beulig, F., Røy, H., McGlynn, S. E., and Jørgensen, B. B.: Cryptic CH_4 cycling in the sulfate-methane transition of marine sediments apparently mediated by ANME-1 archaea, ISME J., 13, 250–262, https://doi.org/10.1038/s41396-018-0273-z, 2018.

Boetius, A., Ravenschlag, K., Schubert, C. J., Rickert, D., Widdel, F., Giesecke, A., Amann, R., Jørgensen, B. B., Witte, U., and Pfannkuche, O.: A marine microbial consortium apparently mediating anaerobic oxidation of methane, Nature, 407, 623–626, 2000.

Boles, J. R., Eichhubl, P., Garven, G., and Chen, J.: Evolution of a hydrocarbon migration pathway along basin-bounding faults: Evidence from fault cement, AAPG Bull., 88, 947–970, 2004.

Cadena, S., García-Maldonado, J. Q., López-Lozano, N. E., and Cervantes, F. J.: Methanogenic and sulfate-reducing activities in a hypersaline microbial mat and associated microbial diversity, Microbial. Ecol., 75, 930–940, 2018.

Canfield, D. E. and Kraft, B.: The "oxygen" in oxygen minimum zones, Environ. Microbiol., 24, 5332–5344, 2022.

Capone, D. G., Bronk, D. A., Mulholland, M. R., and Carpenter, E. J.: Nitrogen in the marine environment, Elsevier, ISBN 978-0-12-372522-6, https://doi.org/10.1016/B978-0-12-372522-6.X0001-1, 2008.

Chistoserdova, L.: Methylotrophs in natural habitats: current insights through metagenomics, Appl. Microbiol. Biot., 99, 5763–5779, 2015.

Conrad, R.: Contribution of hydrogen to methane production and control of hydrogen concentrations in methanogenic soils and sediments, FEMS Microbiol. Ecol., 28, 193–202, 1999.

Conrad, R.: Importance of hydrogenotrophic, aceticlastic and methylotrophic methanogenesis for methane production in terrestrial, aquatic and other anoxic environments: a mini review, Pedosphere, 30, 25–39, 2020.

Dale, A. W., Van Cappellen, P., Aguilera, D., and Regnier, P.: Methane efflux from marine sediments in passive and active margins: Estimations from bioenergetic reaction–transport simulations, Earth Planet. Sc. Lett., 265, 329–344, 2008a.

Dale, A. W., Regnier, P., Knab, N. J., Jørgensen, B. B., and Van Cappellen, P.: Anaerobic oxidation of methane (AOM) in marine sediments from the Skagerrak (Denmark): II. Reaction-transport modeling, Geochim. Cosmochim. Ac., 72, 2880–2894, 2008b.

Dale, A. W., Sommer, S., Lomnitz, U., Montes, I., Treude, T., Liebetrau, V., Gier, J., Hensen, C., Dengler, M., Stolpovsky, K., Bryant, L. D., and Wallmann, K.: Organic carbon production, mineralisation and preservation on the Peruvian margin, Biogeosciences, 12, 1537–1559, https://doi.org/10.5194/bg-12-1537-2015, 2015.

De Anda, V., Chen, L.-X., Dombrowski, N., Hua, Z.-S., Jiang, H.-C., Banfield, J. F., Li, W.-J., and Baker, B. J.: Brockarchaeota, a novel archaeal phylum with unique and versatile carbon cycling pathways, Nat. Commun., 12, 1–12, 2021.

Farag, I. F., Zhao, R., and Biddle, J. F.: "Sifarchaeota," a Novel Asgard Phylum from Costa Rican Sediment Capable of Polysaccharide Degradation and Anaerobic Methylotrophy, Appl. Environ. Microb., 87, e02584-02520, https://doi.org/10.1128/AEM.02584-20, 2021.

Ferdelman, T. G., Lee, C., Pantoja, S., Harder, J., Bebout, B. M., and Fossing, H.: Sulfate reduction and methanogenesis in a Thioploca-dominated sediment off the coast of Chile, Geochim. Cosmochim. Ac., 61, 3065–3079, 1997.

Fernandes, S., Mandal, S., Sivan, K., Peketi, A., and Mazumdar, A.: Biogeochemistry of Marine Oxygen Minimum Zones with Special Emphasis on the Northern Indian Ocean, Systems Biogeochemistry of Major Marine Biomes, John Wiley & Sons, Inc., 1–25, https://doi.org/10.1002/9781119554356.ch1, 2022.

Fischer, P. Q., Sánchez-Andrea, I., Stams, A. J., Villanueva, L., and Sousa, D. Z.: Anaerobic microbial methanol conversion in marine sediments, Environ. Microbiol., 23, 1348–1362, 2021.

Gibb, S. W., Mantoura, R. F. C., Liss, P. S., and Barlow, R. G.: Distributions and biogeochemistries of methylamines and ammonium in the Arabian Sea, Deep-Sea Res. Pt. II, 46, 593–615, 1999.

Hanson, R. S. and Hanson, T. E.: Methanotrophic bacteria, Microbiol. Rev., 60, 439–471, 1996.

Helly, J. J. and Levin, L. A.: Global distribution of naturally occurring marine hypoxia on continental margins, Deep-Sea Res. Pt. I, 51, 1159–1168, 2004.

Hinrichs, K.-U. and Boetius, A.: The anaerobic oxidation of methane: new insights in microbial ecology and biogeochemistry, in: Ocean Margin Systems, edited by: Wefer, G., Billett, D., Hebbeln, D., Jørgensen, B. B., Schlüter, M., and Van Weering, T., Springer-Verlag, Berlin, 457–477, https://doi.org/10.1007/978-3-662-05127-6_28, 2002.

Hoehler, T. M., Alperin, M. J., Albert, D. B., and Martens, C. S.: Apparent minimum free energy requirements for methanogenic Archaea and sulfate-reducing bacteria in an anoxic marine sediment, FEMS Microbiol. Ecol., 38, 33–41, 2001.

Hornafius, J. S., Quigley, D., and Luyendyk, B. P.: The world's most spectacular marine hydrocarbon seeps (Coal Oil Point, Santa Barbara Channel, California): Quantification of emissions, J. Geophys. Res.-Oceans, 104, 20703–20711, 1999.

Joye, S. B., Boetius, A., Orcutt, B. N., Montoya, J. P., Schulz, H. N., Erickson, M. J., and Logo, S. K.: The anaerobic oxidation of methane and sulfate reduction in sediments from Gulf of Mexico cold seeps, Chem. Geol., 205, 219–238, 2004.

Jørgensen, B. B.: A comparison of methods for the quantification of bacterial sulphate reduction in coastal marine sediments: I. Measurements with radiotracer techniques, Geomicrobiol. J., 1, 11–27, 1978.

Jørgensen, B. B.: Bacteria and marine biogeochemistry, in: Marine biogeochemistry, edited by: Schulz, H. D. and Zabel, M., Springer Verlag, Berlin, 173–201, https://doi.org/10.1007/978-3-662-04242-7_5, 2000.

Kallmeyer, J., Ferdelman, T. G., Weber, A., Fossing, H., and Jørgensen, B. B.: A cold chromium distillation procedure for radiolabeled sulfide applied to sulfate reduction measurements, Limnol. Oceanogr.-Meth., 2, 171–180, 2004.

King, G., Klug, M. J., and Lovley, D. R.: Metabolism of acetate, methanol, and methylated amines in intertidal sediments of Lowes Cove, Maine, 45, 1848–1853, 1983.

Kivenson, V., Paul, B. G., and Valentine, D. L.: An ecological basis for dual genetic code expansion in marine deltaproteobacteria, Front. Microbiol., 12, 1545, https://doi.org/10.3389/fmicb.2021.680620, 2021.

Knittel, K. and Boetius, A.: Anaerobic oxidation of methane: progress with an unknown process, Annu. Rev. Microbiol., 63, 311–334, 2009.

Kononets, M., Tengberg, A., Nilsson, M., Ekeroth, N., Hylén, A., Robertson, E. K., Van De Velde, S., Bonaglia, S., Rütting, T., and Blomqvist, S.: In situ incubations with the Gothenburg benthic chamber landers: Applications and quality control, J. Marine Syst., 214, 103475, https://doi.org/10.1016/j.jmarsys.2020.103475, 2021.

Krause, S. J. and Treude, T.: Deciphering cryptic methane cycling: Coupling of methylotrophic methanogenesis and anaerobic oxidation of methane in hypersaline coastal wetland sediment, Geochim. Cosmochim. Ac., 302, 160–174, 2021.

Kristjansson, J. K., Schönheit, P., and Thauer, R. K.: Different Ks values for hydrogen of methanogenic bacteria and sulfate reducing bacteria: an explanation for the apparent inhibition of methanogenesis by sulfate, Arch. Microbiol., 131, 278–282, 1982.

Lee, C. and Olson, B. L.: Dissolved, exchangeable and bound aliphatic amines in marine sediments: initial results, Org. Geochem., 6, 259–263, 1984.

Leifer, I., Kamerling, M. J., Luyendyk, B. P., and Wilson, D. S.: Geologic control of natural marine hydrocarbon seep emissions, Coal Oil Point seep field, California, Geo-Mar. Lett., 30, 331–338, 2010.

Levin, L.: Oxygen minimum zone benthos: Adaptation and community response to hypoxia, Oceanogr. Mar. Biol., 41, 1–45, 2003.

Levin, L. A., Ekau, W., Gooday, A. J., Jorissen, F., Middelburg, J. J., Naqvi, S. W. A., Neira, C., Rabalais, N. N., and Zhang, J.: Effects of natural and human-induced hypoxia on coastal benthos, Biogeosciences, 6, 2063–2098, https://doi.org/10.5194/bg-6-2063-2009, 2009.

Lovley, D. R. and Klug, M. J.: Model for the distribution of sulfate reduction and methanogenesis in freshwater sediments, Geochim. Cosmochim. Ac., 50, 11–18, 1986.

Lyu, Z., Shao, N., Akinyemi, T., and Whitman, W. B.: Methanogenesis, Curr. Biol., 28, R727–R732, 2018.

Maltby, J., Sommer, S., Dale, A. W., and Treude, T.: Microbial methanogenesis in the sulfate-reducing zone of surface sediments traversing the Peruvian margin, Biogeosciences, 13, 283–299, https://doi.org/10.5194/bg-13-283-2016, 2016.

Maltby, J., Steinle, L., Löscher, C. R., Bange, H. W., Fischer, M. A., Schmidt, M., and Treude, T.: Microbial methanogenesis in the sulfate-reducing zone of sediments in the Eckernförde Bay, SW Baltic Sea, Biogeosciences, 15, 137–157, https://doi.org/10.5194/bg-15-137-2018, 2018.

Mausz, M. A. and Chen, Y.: Microbiology and ecology of methylated amine metabolism in marine ecosystems, Curr. Issues Mol. Biol., 33, 133–148, 2019.

Michaelis, W., Seifert, R., Nauhaus, K., Treude, T., Thiel, V., Blumenberg, M., Knittel, K., Gieseke, A., Peterknecht, K., Pape, T., Boetius, A., Aman, A., Jørgensen, B. B., Widdel, F., Peckmann, J., Pimenov, N. V., and Gulin, M.: Microbial reefs in the Black Sea fueled by anaerobic oxidation of methane, Science, 297, 1013–1015, 2002.

Middelburg, J. J. and Levin, L. A.: Coastal hypoxia and sediment biogeochemistry, Biogeosciences, 6, 1273–1293, https://doi.org/10.5194/bg-6-1273-2009, 2009.

Moretti, I.: The role of faults in hydrocarbon migration, Petrol. Geosci., 4, 81–94, 1998.

Nauhaus, K., Albrecht, M., Elvert, M., Boetius, A., and Widdel, F.: In vitro cell growth of marine archaeal-bacterial consortia during anaerobic oxidation of methane with sulfate, Environ. Microbiol., 9, 187–196, 2007.

Oremland, R. S. and Polcin, S.: Methanogenesis and sulfate reduction: competitive and noncompetitive substrates in estuarine sediments, Appl. Environ. Microb., 44, 1270–1276, 1982.

Oremland, R. S. and Taylor, B. F.: Sulfate reduction and methanogenesis in marine sediments, Geochim. Cosmochim. Ac., 42, 209–214, 1978.

Oremland, R. S., Marsh, L. M., and Polcin, S.: Methane production and simultaneous sulphate reduction in anoxic, salt marsh sediments, Nature, 296, 143–145, 1982.

Oren, A.: Formation and breakdown of glycine betaine and trimethylamine in hypersaline environments, Antonie van Leeuwenhoek, 58, 291–298, 1990.

Orphan, V. J., Hinrichs, K.-U., Ussler III, W., Paull, C. K., Tayleor, L. T., Sylva, S. P., Hayes, J. M., and DeLong, E. F.: Comparative analysis of methane-oxidizing archaea and sulfate-reducing bacteria in anoxic marine sediments, Appl. Environ. Microb., 67, 1922–1934, 2001.

Paulmier, A. and Ruiz-Pino, D.: Oxygen minimum zones (OMZs) in modern ocean, Progr. Oceanogr., 80, 113–128, 2009.

Qin, Q., Kinnaman, F. S., Gosselin, K. M., Liu, N., Treude, T., and Valentine, D. L.: Seasonality of water column methane oxidation and deoxygenation in a dynamic marine environment, Geochim. Cosmochim. Ac., 336, 219–230, 2022.

Ragsdale, S. W. and Pierce, E.: Acetogenesis and the Wood–Ljungdahl pathway of CO_2 fixation, Biochimica et Biophysica Acta (BBA)-Proteins and Proteomics, 1784, 1873–1898, 2008.

Reeburgh, W. S.: Oceanic methane biogeochemistry, Chem. Rev., 107, 486–513, 2007.

Reimers, C. E., Ruttenberg, K. C., Canfield, D. E., Christiansen, M. B., and Martin, J. B.: Porewater pH and authigenic phases formed in the uppermost sediments of Santa Barbara Basin, Geochim. Cosmochim. Ac., 60, 4037–4057, 1996.

Rullkötter, J.: Organic matter: the driving force for early diagenesis, in: Marine geochemistry, Springer, 125–168, IBSN 13 978-3-540-32143-9, 2006.

Schimmelmann, A. and Kastner, M.: Evolutionary changes over the last 1000 years of reduced sulfur phases and organic carbon in varved sediments of the Santa Barbara Basin, California, Geochim. Cosmochim. Ac., 57, 67–78, 1993.

Sholkovitz, E.: Interstitial water chemistry of the Santa Barbara Basin sediments, Geochim. Cosmochim. Ac., 37, 2043–2073, 1973.

Smeraglia, L., Fabbi, S., Billi, A., Carminati, E., and Cavinato, G. P.: How hydrocarbons move along faults: Evidence from microstructural observations of hydrocarbon-bearing carbonate fault rocks, Earth Planet. Sc. Lett., 584, 117454, https://doi.org/10.1016/j.epsl.2022.117454, 2022.

Sousa, D. Z., Visser, M., Van Gelder, A. H., Boeren, S., Pieterse, M. M., Pinkse, M. W., Verhaert, P. D., Vogt, C., Franke, S., and Kümmel, S.: The deep-subsurface sulfate reducer Desulfotomaculum kuznetsovii employs two methanol-degrading pathways, Nat. Commun., 9, 1–9, 2018.

Soutar, A. and Crill, P. A.: Sedimentation and climatic patterns in the Santa Barbara Basin during the 19th and 20th centuries, Geol. Soc. Am. Bull., 88, 1161–1172, 1977.

Stephenson, M. and Stickland, L. H.: CCVII. Hydrogenase. III. The bacterial formation of methane by the reduction of one-carbon compounds by molecular hydrogen, Biochem. J., 27, 1517–1527, 1933.

Taubert, M., Grob, C., Howat, A. M., Burns, O. J., Pratscher, J., Jehmlich, N., von Bergen, M., Richnow, H. H., Chen, Y., and Murrell, J. C.: Methylamine as a nitrogen source for microorganisms from a coastal marine environment, Environ. Microbiol., 19, 2246–2257, 2017.

Thauer, R. K.: Biochemistry of methanogenesis: a tribute to Marjory Stephenson, Microbiology, 144, 2377–2406, 1998.

Treude, T.: Biogeochemical reactions in marine sediments underlying anoxic water bodies, in: Anoxia: Paleontological Strategies and Evidence for Eukaryote Survival, edited by: Altenbach, A., Bernhard, J., and Seckbach, J., Cellular Origins, Life in Extreme Habitats and Astrobiology (COLE) Book Series, Springer, Dordrecht, 18–38, https://doi.org/10.1007/978-94-007-1896-8_2, 2011.

Treude, T. and Valentine, D. L.: Porewater geochemistry of sediments collected Fall 2019 in the Santa Barbara Basin using ROV Jason during R/V *Atlantis* cruise AT42-19, Version 1, Biological and Chemical Oceanography Data Management Office (BCO-DMO) [data set], https://doi.org/10.26008/1912/bco-dmo.867007.1, 2022a.

Treude, T. and Valentine, D. L.: Porosity and density of sediments collected Fall 2019 in the Santa Barbara Basin using ROV Jason during R/V *Atlantis* cruise AT42-19, Version 1, Biological and Chemical Oceanography Data Management Office (BCO-DMO) [data set], https://doi.org/10.26008/1912/bco-dmo.867113.1, 2022b.

Treude, T. and Valentine, D. L.: Microbial activity from sediments collected Fall 2019 in the Santa Barbara Basin using ROV Jason during R/V *Atlantis* cruise AT42-19, Version 1, Biological and Chemical Oceanography Data Management Office (BCO-DMO) [data set], https://doi.org/10.26008/1912/bco-dmo.867221.1, 2022c.

Treude, T., Krüger, M., Boetius, A., and Jørgensen, B. B.: Environmental control on anaerobic oxidation of methane in the gassy sediments of Eckernförde Bay (German Baltic), Limnol. Oceanogr., 50, 1771–1786, 2005.

Treude, T., Smith, C. R., Wenzhoefer, F., Carney, E., Bernardino, A. F., Hannides, A. K., Krueger, M., and Boetius, A.: Biogeochemistry of a deep-sea whale fall: sulfate reduction, sulfide efflux and methanogenesis, Mar. Ecol.-Prog. Ser., 382, 1–21, 2009.

Wang, X.-c. and Lee, C.: The distribution and adsorption behavior of aliphatic amines in marine and lacustrine sediments, Geochim. Cosmochim. Ac., 54, 2759–2774, 1990.

Wang, X.-C. and Lee, C.: Adsorption and desorption of aliphatic amines, amino acids and acetate by clay minerals and marine sediments, Mar. Chem., 44, 1–23, 1993.

Wang, X.-C. and Lee, C.: Sources and distribution of aliphatic amines in salt marsh sediment, Org. Geochem., 22, 1005–1021, 1994.

Wehrmann, L. M., Risgaard-Petersen, N., Schrum, H. N., Walsh, E. A., Huh, Y., Ikehara, M., Pierre, C., D'Hondt, S., Ferdelman, T. G., and Ravelo, A. C.: Coupled organic and inorganic carbon cycling in the deep subseafloor sediment of the northeastern Bering Sea Slope (IODP Exp. 323), Chem. Geol., 284, 251–261, 2011.

Wilfert, P., Krause, S., Liebetrau, V., Schönfeld, J., Haeckel, M., Linke, P., and Treude, T.: Response of anaerobic methanotrophs and benthic foraminifera to 20 years of methane emission from a gas blowout in the North Sea, Mar. Petrol. Geol., 68, 731–742, 2015.

Winfrey, M. R. and Ward, D. M.: Substrates for sulfate reduction and methane production in i ntertidal sediments, Appl. Environ. Microb., 45, 193–199, 1983.

Working Group on California Earthquake Probabilities: Seismic hazards in Southern California: Probable earthquakes, 1994 to 2024, B. Seismol. Soc. Am., 85, 379–439, 1995.

Wright, J. J., Konwar, K. M., and Hallam, S. J.: Microbial ecology of expanding oxygen minimum zones, Nat. Rev. Microbiol., 10, 381–394, 2012.

Wyrtki, K.: The oxygen minima in relation to ocean circulation, Deep Sea Research and Oceanographic Abstracts, 9, 11–23, https://doi.org/10.1016/0011-7471(62)90243-7, 1962.

Xiao, K., Beulig, F., Kjeldsen, K., Jorgensen, B., and Risgaard-Petersen, N.: Concurrent Methane Production and Oxidation in Surface Sediment from Aarhus Bay, Denmark, Front. Microbiol., 8, 1198, https://doi.org/10.3389/fmicb.2017.01198, 2017.

Xiao, K., Beulig, F., Roy, H., Jorgensen, B., and Risgaard-Petersen, N.: Methylotrophic methanogenesis fuels cryptic methane cycling in marine surface sediment, Limnol. Oceanogr., 63, 1519–1527, 10.1002/lno.10788, 2018.

Xiao, K.-Q., Moore, O. W., Babakhani, P., Curti, L., and Peacock, C. L.: Mineralogical control on methylotrophic methanogenesis and implications for cryptic methane cycling in marine surface sediment, Nat. Commun., 13, 1–9, 2022.

Zhuang, G.-C., Elling, F. J., Nigro, L. M., Samarkin, V., Joye, S. B., Teske, A., and Hinrichs, K.-U.: Multiple evidence for methylotrophic methanogenesis as the dominant methanogenic pathway in hypersaline sediments from the Orca Basin, Gulf of Mexico, Geochim. Cosmochim. Ac., 187, 1–20, 2016.

Zhuang, G.-C., Montgomery, A., and Joye, S. B.: Heterotrophic metabolism of C1 and C2 low molecular weight compounds in northern Gulf of Mexico sediments: Controlling factors and implications for organic carbon degradation, Geochim. Cosmochim. Ac., 247, 243–260, 2019.

Zhuang, G.-C., Lin, Y.-S., Bowles, M. W., Heuer, V. B., Lever, M. A., Elvert, M., and Hinrichs, K.-U.: Distribution and isotopic composition of trimethylamine, dimethylsulfide and dimethylsulfoniopropionate in marine sediments, Mar. Chem., 196, 35–46, 2017.

Zhuang, G.-C., Heuer, V. B., Lazar, C. S., Goldhammer, T., Wendt, J., Samarkin, V. A., Elvert, M., Teske, A. P., Joye, S. B., and Hinrichs, K.-U.: Relative importance of methylotrophic methanogenesis in sediments of the Western Mediterranean Sea, Geochim. Cosmochim. Acta, 224, 171–186, 2018.